

Interaction-mediated asymmetries of the quantized Hall effect

A. SIDDIKI^{1,2(a)}, J. HORAS¹, J. MOSER¹, W. WEGSCHEIDER³ and S. LUDWIG¹

¹ *Physics Department, Arnold Sommerfeld Center for Theoretical Physics, and Center for NanoScience, Ludwig-Maximilians-Universität - Theresienstrasse 37, 80333 Munich, Germany, EU*

² *Physics Department, Faculty of Arts and Sciences, Muğla University - 48170-Kötekli, Muğla, Turkey*

³ *Institut für Experimentelle und Angewandte Physik, Universität Regensburg - D-93040 Regensburg, Germany, EU*

received 30 July 2009; accepted 22 September 2009

published online 23 October 2009

PACS 73.43.Cd – Theory and modelling

PACS 73.43.Fj – Novel experimental methods; measurements

PACS 73.43.-f – Quantum Hall effects

Abstract – Experimental and theoretical investigations on the integer quantized Hall effect in gate-defined narrow Hall bars are presented. At low electron mobility the classical (high-temperature) Hall resistance line $R_H(B)$ cuts through the center of all Hall plateaus. In contrast, for our high-mobility samples the intersection point, at even filling factors $\nu = 2, 4, \dots$, is clearly shifted towards larger magnetic fields B . This asymmetry is in good agreement with predictions of the screening theory, *i.e.* taking Coulomb interaction into account. The observed effect is directly related to the formation of incompressible strips in the Hall bar. The spin-split plateau at $\nu = 1$ is found to be almost symmetric regardless of the mobility. We explain this within the so-called effective g -model.

Copyright © EPLA, 2009

The integer quantized Hall effect (IQHE) can be observed when a two-dimensional electron system (2DES) at low temperature is subjected to a strong magnetic field B normal to the plane of the 2DES. The relevance of the IQHE stems from its universal features. Most prominent are the precise values $R_H = h/Ne^2$ (with Planck's constant h , the elementary charge e , and a natural number $N = 1, 2, \dots$) the quantized Hall resistance takes on the Hall plateaus while at the same time the longitudinal resistance R_L vanishes [1]. These main characteristics of the IQHE are well established in experiments as well as within single-particle theories [1–3]. However, these conventional theories do not provide a full understanding of all features observed in magneto-resistance experiments. A comprehensive model needs to take into account the Coulomb interaction between charge carriers [4], which is a subject of ongoing investigations [5–7].

In the classical (high-temperature) limit the Hall resistance $R_H(B)$ resembles a straight line described by $R_H(B) = h/\nu_0(B)e^2$ with $\nu_0(B)$ being the filling factor averaged across the Hall bar width. The local filling factor is defined as $\nu(B, x) = n_s(x, B)/n_\phi(x, B)$, where n_s and $n_\phi \propto B$ are the local number densities of electrons and magnetic flux quanta in the 2DES. In most experiments

reported, the Hall plateaus of $R_H(B)$ extend symmetrically in respect to integer values of $\nu_0 \equiv N = 1, 2, \dots$. In other words the classical Hall line $R_H(B)$ cuts through the center of each plateau [8]. Exceptions from such symmetric plateaus have been observed on etched narrow Hall bars in the limit of low mobility [9,10]. The experimental results reported in ref. [10] have been described within single particle theories [2,3] making additional assumptions about the disorder potential, namely by comparison of the electron diffusion length and the sample width [10]. In earlier experiments asymmetric plateaus were attributed to interactions [9], which is in agreement with the recent experimental [11] and theoretical [12] findings.

We present investigations on the IQHE as a function of mobility and temperature employing narrow Hall bars. Our devices are electrostatically defined by top gates, allowing for very smooth edges of the Hall bar. The Hall plateaus at even filling factors develop a pronounced asymmetry while temperature is decreased. This asymmetry is observed only at high mobilities, where the electron mean-free path (l_{mfp}) exceeds the Hall bar width. Hence, we can exclude disorder as the origin in contrast to ref. [10]. Considering the Coulomb interaction between electrons our results are qualitatively explained using self-consistent (SC) calculations [13,14]. The model

^(a)E-mail: siddiki@mu.edu.tr

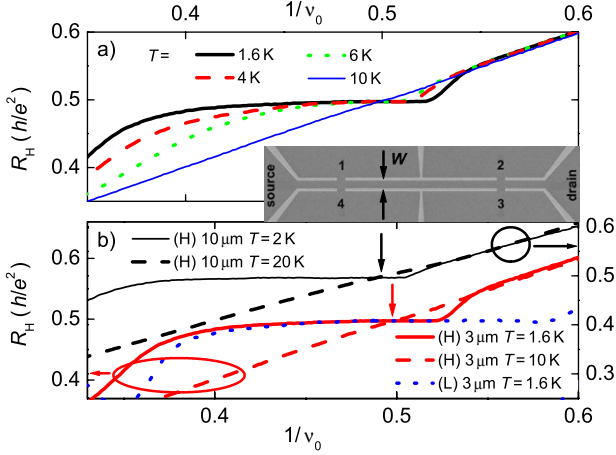


Fig. 1: (Color online) (a) Measured Hall resistance of the higher-mobility wafer at a Hall bar width $W = 3 \mu\text{m}$ for several temperatures as a function of the averaged reciprocal filling factor at the $\nu_0 = 2$ plateaus. Inset: scanning electron micrograph of the gate layout. Metal gates are light gray. Ohmic contacts source and drain carry the current while 1–4 are voltage probes. (b) Hall resistances in the limit of high and low temperatures of the higher-mobility wafer (H) at $W = 10 \mu\text{m}$ and $W = 3 \mu\text{m}$ and of the lower-mobility wafer (L) at $W = 3 \mu\text{m}$.

predicts an interaction-induced asymmetric density of states (DOS) for charge carriers within the Landau levels [15].

The experiments presented here are performed on two similar GaAs/AlGaAs heterostructures both containing a 2DES 110 nm below the surface. The low-temperature charge carrier densities and mobilities of the two wafers are $n_{s1} \simeq 2.8 \times 10^{15} \text{ m}^{-2}$, $n_{s2} \simeq 1.8 \times 10^{15} \text{ m}^{-2}$, $\mu_1 \simeq 140 \text{ m}^2/\text{Vs}$ ($l_{\text{mfp}} \approx 12 \mu\text{m}$), and $\mu_2 \simeq 300 \text{ m}^2/\text{Vs}$ ($l_{\text{mfp}} \approx 21 \mu\text{m}$). A typical gate layout processed by electron beam lithography is displayed in the inset to fig. 1(a). All gates of a sample are biased with the same negative voltage to locally deplete the 2DES beneath the gates and thus define the Hall bar. Measurements of the Hall resistance R_H are carried out using the contacts 1-3 (or 2-4) as voltage probes. Likewise contacts 1-2 (or 3-4) serve to measure the longitudinal resistance R_L .

Figure 1(a) displays R_H as a function of $1/\nu_0$ ($\propto B$) in the $\nu_0 \simeq 2$ range for temperatures between $1.6 \text{ K} \leq T \leq 10 \text{ K}$ measured on the higher-mobility wafer at a Hall bar width of $W = 3 \mu\text{m}$. At $T = 10 \text{ K}$ we find the classically expected straight line and, as the temperature is decreased, the Hall plateau at $\nu_0 = 2$ develops. Noticeably, the plateau grows stronger on the low-magnetic-field side ($\nu_0 > 2$), ultimately resulting in an asymmetric plateau at low temperatures. Figure 1(b) displays $R_H(1/\nu_0)$ in the region of the $\nu_0 \simeq 2$ plateau measured on both wafers for $W = 10 \mu\text{m}$ and $W = 3 \mu\text{m}$ at temperatures $T \lesssim 2 \text{ K}$ as well as $T \gtrsim 10 \text{ K}$. For the lower-mobility wafer the classical high-temperature line cuts roughly through the center of the plateau as expected in single-particle models [2,3].

In contrast, for the higher mobility we again find asymmetric plateaus. This behavior is likewise for larger even filling factors (not shown). The main experimental observations can be summarized as follows: i) in the limit of high-mobility Hall plateaus in narrow gate-defined bars are asymmetric in respect to the classical R_H line. ii) As the mobility is reduced the conventional symmetric plateaus are recovered. This makes disorder unlikely as possible origin of the observed asymmetry. Instead, we consider the Coulomb interaction between electrons. In the following a SC model is briefly introduced [13]. We start from the single particle Hamiltonian but then explicitly include the Coulomb interaction.

Consider an electron with charge e , effective mass m^* , and momentum \mathbf{p} moving in a time-independent potential $V_{\text{ext}}(\mathbf{r})$, generated by the top gates as well as ionized donors and other defects. In a magnetic field B oriented perpendicular to the 2DES described by the vector potential $\mathbf{A}(\mathbf{r})$ (in an appropriate gauge) the Hamilton operator reads

$$H = \frac{(\mathbf{p} - e\mathbf{A}(\mathbf{r}))^2}{2m^*} + V_{\text{ext}}(\mathbf{r}) + V_{e-e}(\mathbf{r}) + \sigma g^* \mu_B B. \quad (1)$$

The potential $V_{e-e}(\mathbf{r})$ accounts for Coulomb interactions between electrons with spin $\sigma = \pm 1/2$, where g^* is the Lande g -factor and μ_B Bohr's magneton. We assume i) translational invariance in the y -direction along the Hall bar [16], ii) that all charge carriers reside on the $z = 0$ plane [4], iii) that disorder induces a mobility-dependent short-range broadening of the DOS, $D(E)$, with scattering parameter Γ [13], and iv) that the electrostatic potential varies weakly on the scale of the magnetic length $l_B = \sqrt{\hbar/eB}$. Assumptions i) and ii) allow to reduce the position vector to the lateral coordinate across the Hall bar ($\mathbf{r} = (x, y, z) \rightarrow (x, y_0, 0) \rightarrow x$). We replace the actual wave functions of the electrons with delta functions and apply the Thomas-Fermi approximation [17] neglecting the spin degree of freedom ($g^* = 0$) resulting in the carrier density

$$n_s(x) = \int dE D(E) \left[e^{\frac{E - \mu(x)}{k_B T}} + 1 \right]^{-1}. \quad (2)$$

To obtain local conductivities we perform a spatial averaging over the Fermi wavelength ($\sim 33 \text{ nm}$) simulating the finite extent of the wave functions, thus, relaxing the strict locality of our model. The electrochemical potential $\mu(x) = \mu_{\text{eq}}^* - V(x)$ is composed of the equilibrium chemical potential μ_{eq}^* and the total potential energy, containing both the Coulomb interaction between electrons and the external potential defining the Hall bar

$$V(x) = V_{\text{ext}}(x) + V_{e-e}(x) = \frac{2e^2}{\kappa} \int_{-d}^d [n_0 - n_s(\tilde{x})] K(x, \tilde{x}) d\tilde{x}, \quad (3)$$

expressed via a Kernel $K(x, \tilde{x})$ [13] such that $V(-d) = V(d) = 0$ (at the Hall bar boundaries). Here $2d < W$ is

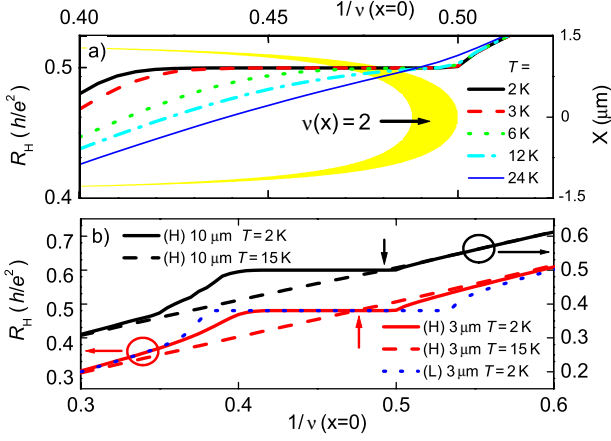


Fig. 2: (Color online) (a) Calculated Hall resistance for high mobility (H) and $W = 3 \mu\text{m}$ plotted for several temperatures as a function of the reciprocal center filling factor $1/\nu(x=0)$. The shaded region (yellow) corresponds to the calculated spatial distribution of the IS with $\nu(B, x) = 2$ across the Hall bar (rhs axis $0 \leq x \leq W$). (b) Hall resistances as in fig. 1(b) but calculated assuming that the biased gates result in an edge depletion of $W/2 - d = 80 \text{ nm}$. The donor density is taken to be $4 \times 10^{15} \text{ m}^{-2}$, resulting in realistic Fermi energies of $E_F = 11.9 \text{ meV}$ (13.4 meV) for $W = 3 \mu\text{m}$ ($10 \mu\text{m}$).

the reduced sample width, taking into account the lateral depletion beneath the top gates, κ is the average dielectric constant, and n_0 the constant (and homogeneous) effective donor number density. Equations (2) and (3) complete our SC problem, which we solve iteratively to obtain electrostatic quantities, such as the local electric field $\mathbf{E}(x)$.

Assuming a constant current $I = \int_{-d}^d j_y(x, y) dx$ along the Hall bar, that is in y -direction, the local current density $\mathbf{j}(x)$ results from Ohm's law

$$\nabla \mu(x)/e \equiv \mathbf{E}(x) = \hat{\rho}(x) \mathbf{j}(x), \quad (4)$$

where the resistivity tensor $\hat{\rho}(x)$ is obtained from the DOS [13,17] and taking into account short-range potential fluctuations [14]. From $\nabla \cdot \mathbf{j}(x) = 0$ and $\nabla \times \mathbf{E}(x) = 0$ and utilizing the translational invariance one obtains

$$j_x = 0, \quad E_y(x) = E_y^0 \equiv I \int_{-d}^d \frac{dx}{\rho_L(x)}, \quad (5)$$

$$j_y(x) = E_y^0 / \rho_L(x), \quad E_x(x) = E_y^0 \rho_H(x) / \rho_L(x),$$

where $\rho_L(x)$ and $\rho_H(x)$ are the diagonal and off-diagonal entries of the resistivity tensor, respectively, and E_y^0 is a constant electric field oriented in the y -direction. For a given current eq. (5) leads to the global resistances

$$R_H = \frac{V_H}{I} = \frac{E_y^0}{I} \int_{-d}^d dx \frac{\rho_H(x)}{\rho_L(x)}, \quad R_L = \frac{2dE_y^0}{I}, \quad (6)$$

where the electron temperature enters via eq. (2).

Figure 2(a) presents $R_H(B)$ of a Hall bar of width $W = 3 \mu\text{m}$ calculated in the limit of high mobility (assuming a mean-free path large compared to $2d \lesssim W$) as a

function of a magnetic field perpendicular to the 2DES for several temperatures $2 \text{ K} \leq T \leq 24 \text{ K}$. Within an incompressible strip (IS) the carrier density $n_s(B, x)$ and, thus, the local filling factor $\nu(B, x)$ are constant. In fig. 2(a) the IS with $\nu(B, x) = 2$ is highlighted depicted by a shaded region (yellow). Here we display the bare IS neglecting broadening of the adjacent compressible regions caused by temperature or the quantum-mechanical extension of the electron wave functions. At its high magnetic-field end (bulk region) the IS is extended over most of the sample width. As the B -field is reduced the IS splits into two edge channels. Let us first consider the low-temperature limit of the local resistivity tensor. Away from the IS (white background in fig. 2(a)) the compressible 2DES behaves like a metal with finite diagonal elements ρ_L and ρ_H taking a value close to its classical (high-temperature) limit. However, within an IS backscattering is absent, hence $\rho_L(\nu = N) = 0$ and $\rho_H(\nu = N) = \frac{h}{Ne^2}$ takes its quantized value. Accordingly, whenever somewhere across the Hall bar an IS exists $E_y^0 = 0$, and eq. (6) yields $R_L = 0$ and a Hall plateau with $R_H = \rho_H(\nu = N) = \frac{h}{Ne^2}$. The calculated temperature dependence $R_H(T)$ shown in fig. 2(a) is a consequence of the broadening of the Fermi distribution function with increasing temperature. Simply speaking, a broader Fermi distribution results in a wider transition between compressible and incompressible regions, melting an IS from its edges. Hence, with increasing temperature an IS and the according Hall plateau disappear first where the bare IS is narrow, hence on its low-magnetic-field side (compare with fig. 2(a)). On the other hand, the large (bulk) region of an IS at its high-magnetic-field end withstands much higher temperatures. As a direct consequence, the intersection point of the classical (high-temperature) R_H line with a Hall plateau is determined by the widest part of an IS.

Figure 2(b) displays calculated R_H curves as a function of $1/\nu_0$ for the same two Hall bar widths as the actually measured devices have (compare with fig. 1). For the wider sample the two cases of a mean-free path much larger (high-mobility limit) or smaller (low-mobility limit) than the bar width are presented. Long-range potential fluctuations originating from charged impurities and resulting in a finite mobility, are simulated by modulating the external potential $V_{\text{ext}}(x) \rightarrow V_{\text{ext}}(x) + V_{\text{mod}} \cos(m_p \pi x/d)$, where m_p defines the mobility [14]. For the low-mobility limit we chose the period $2d/m_p \pi = 1200 \text{ nm}$ and a strong modulation of $V_{\text{mod}} \simeq E_F/5$ [14]. The result are disorder broadened ISs consisting of bulk regions which extend more symmetrically in both magnetic-field directions centered at the integer filling factors $\nu_0 = N$. Consequently, for a low mobility also the Hall plateaus are almost symmetrically extended in respect to the intersection point with the classical R_H line, being independent of mobility.

The SC calculations presented in fig. 2 show excellent qualitative agreement with the measured data displayed in fig. 1. Our analysis indicates that the asymmetric Hall plateaus measured in the limit of high mobility and narrow

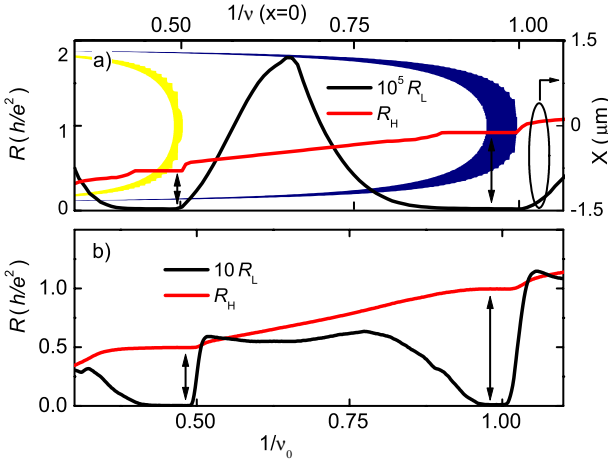


Fig. 3: (Color online) (a) Spatial distribution of the ISs with $\nu(B, x) = 1$ (dark, blue) and $\nu(B, x) = 2$ (shaded region, yellow) as a function of $1/\nu(x=0)$, calculated in the effective g -factor model. Also shown are R_H and R_L curves calculated in the high-mobility limit for $T = 1.6$ K and $W = 3 \mu\text{m}$. (b) Measured $R_H(1/\nu_0)$ and $R_L(1/\nu_0)$ for the higher-mobility wafer and $W = 3 \mu\text{m}$. The widest extensions of the ISs are marked by arrows.

gate-defined Hall bars, can be explained by the interaction between charge carriers resulting in the formation of ISs. At high mobility the Hall resistance is quantized as long as there exists an IS wide compared to the Fermi wavelength. The long extension of the measured Hall plateaus to the low-field side of the intersection with the classical Hall line allows us to conclude, that in narrow Hall bars with high mobility and smooth (gate-defined) edges the edge potential profile rather than disorder dominates the IQHE. When decreasing the mobility our measurements and calculations show a transition to symmetric Hall plateaus, indicating that in this case disorder extends the large bulk region of the ISs in both field directions resulting in symmetric plateaus. Our numerical calculations suggest that the period $2d/m_p\pi$ defines the long-range length scale of the disorder potential and, thus, compared to the sample width is a measure of the mobility, suggesting a low mobility for $1/m_p\pi \ll 1$.

It is known that exchange correlation effects cause a spin-split DOS usually expressed in a strongly enhanced effective g -factor g^* [18]. This enhancement is expected to be even aggravated within ISs. We include the spin degree of freedom in our model in a phenomenological manner described in ref. [19]. While the exact value of g^* is not a determining parameter for our calculations, only a large enough gap of the DOS $\Delta E_Z \gg k_B T$ results in the formation of spin-split ISs. Recent theoretical investigations, within the self-consistent Thomas-Fermi-Dirac approximation, provide strong support to our approach in handling the exchange enhancement of the effective g^* [20]

Figure 3(a) presents the calculated spacial distributions of the bare ISs with $\nu = 1$ (dark, blue) and $\nu = 2$

(light, yellow) together with R_H and R_L as a function of $1/\nu_0$. The corresponding measured $R_H(1/\nu_0)$ and $R_L(1/\nu_0)$ curves (for the higher mobility) are displayed in fig. 3(b). To calculate R_L in the high-mobility limit we used a phenomenological model proposed by Gerhardtts and Gross [21]. An IS vanishes whenever the adjacent compressible regions overlap, that is either when the quantum-mechanical wavelength of the electrons exceed its widths or when the thermal energy $\sim k_B T$ exceeds the local potential drop. The latter is given by $g^* \mu_B B$ for $\nu = 1$ or $\hbar\omega_c - g^* \mu_B B$ for even filling factors. Where an IS exists $R_L = 0$ (and $R_H = \text{const}$). In our specific case the two ISs do not coexist at any magnetic field value. The IS at $\nu = 1$ is more strongly developed and its bulk region extended over a larger B -field interval compared to the IS at $\nu = 2$. Arrows in fig. 3 indicate the $1/\nu$ -values where the ISs are widest, *i.e.* where the classical Hall-line intersects with the Hall plateau. Clearly, the stronger developed IS at $\nu = 1$ results in a more symmetric Hall plateau compared to the even filling factor $\nu = 2$. Showing excellent agreement, the same qualitative behavior is observed in the measured data in fig. 3(b).

In conclusion, we have investigated the IQHE on gate-defined narrow Hall bars at various mobilities and temperatures. At high mobilities and low temperatures we observe asymmetric Hall plateaus in respect to the intersection point with the classical Hall resistance line. Our experimental findings are in excellent agreement with predictions of the screening theory of the IQHE. In contrast to the asymmetric plateaus at even filling factors the measured spin-split plateau at $\nu = 1$ is almost symmetric. This is approved by model calculations within the effective g -factor model.

We thank K. VON KLITZING, R. R. GERHARDTS, and K. IKUSHIMA for stimulating discussions. Financial support by the German Science Foundation via the Germany Israel program DIP and the German Excellence Initiative via the ‘‘Nanosystems Initiative Munich (NIM)’’ is gratefully acknowledged.

REFERENCES

- [1] V. KLITZING, DORDA G. and PEPPER M., *Phys. Rev. Lett.*, **45** (1980) 494.
- [2] LAUGHLIN R. B., *Phys. Rev. B*, **23** (1981) 5632.
- [3] BÜTTIKER M., *Phys. Rev. Lett.*, **57** (1986) 1761.
- [4] CHKLOVSKII D. B., SHKLOVSKII B. I. and GLAZMAN L. I., *Phys. Rev. B*, **46** (1992) 4026.
- [5] GERHARDTS R. R., *Phys. Status Solidi (b)*, **245** (2008) 378.
- [6] ARSLAN S., CICEK E., EKSI D., AKTAS S., WEICHELBAUM A. and SIDDIKI A., *Phys. Rev. B*, **78** (2008) 125423.
- [7] SIDDIKI A., *EPL*, **87** (2009) 17008.
- [8] MATTHEWS J. and CAGE M. E., *J. Res. Natl. Inst. Stand. Technol.*, **110** (2005) 497.
- [9] ZHENG H. Z., CHOI K. K., TSUI D. C. and WEIMANN G., *Phys. Rev. Lett.*, **55** (1985) 1144.

-
- [10] HAUG R. J., v. KLITZING K. and PLOOG K., *Phys. Rev. B*, **35** (1987) 5933.
- [11] HORAS J., SIDDIKI A., MOSER J., WEGSCHEIDER W. and LUDWIG S., *Physica E*, **40** (2008) 1130.
- [12] SAKIROGLU S., ERKARSLAN U., OYLUMLUOGLU G., SIDDIKI A. and SOKMEN I., arXiv:0906.0661 [cond-mat.mes-hall] (2009).
- [13] SIDDIKI A. and GERHARDTS R. R., *Phys. Rev. B*, **70** (2004) 195335.
- [14] SIDDIKI A. and GERHARDTS R. R., *Int. J. Mod. Phys. B*, **21** (2007) 1362.
- [15] HAUG R. J., GERHARDTS R. R., v. KLITZING K. and PLOOG K., *Phys. Rev. Lett.*, **59** (1987) 1349.
- [16] LIER K. and GERHARDTS R. R., *Phys. Rev. B*, **50** (1994) 7757.
- [17] GÜVEN K. and GERHARDTS R. R., *Phys. Rev. B*, **67** (2003) 115327.
- [18] KHRAPAI V. S., SHASHKIN A. A., SHANGINA E. L., PELLEGRINI V., BELTRAM F., BIASIOL G. and SORBA L., *Phys. Rev. B*, **72** (2005) 035344.
- [19] SIDDIKI A., *Physica E*, **40** (2008) 1124.
- [20] BILGEC G., USTUNEL TOFFOLI H., SIDDIKI A. and SOKMEN I., arXiv:0906.0059 [cond-mat.mes-hall] (2009).
- [21] GROSS J. and GERHARDTS R. R., *Physica B*, **256-258** (1998) 60.